Characterization of CdS films prepared by chemical-bath deposition

2000 J. Phys.: Condens. Matter 12 8745

(http://iopscience.iop.org/0953-8984/12/40/316)

J. Phys.: Condens. Matter **12** (2000) 8745–8755. Printed in the UK PII: S0953-8984(00)13510-6

Characterization of CdS films prepared by chemical-bath deposition

A E Rakhshani† and A S Al-Azab

Physics Department, College of Science, Kuwait University, PO Box 5969, Safat 1360, Kuwait

E-mail: rakhshani@kuc01.kuniv.edu.kw

Received 25 April 2000, in final form 11 August 2000

Abstract. Thin films of cadmium sulphide were deposited on glass substrates by the chemical bath deposition method. The results of measurements on the spectral response of photoconductivity, the optical absorption coefficient and the x-ray diffraction were used for the characterization of films. This study revealed that CdS films have tensile strain along the hexagonal (002) planes. The dependence of strain on the grain size is responsible for the variation of energy bandgap with the film thickness. Annealing in air, and at a temperature greater than 150 °C, relaxes the strain, reduces the extent of disorder in grain boundaries, reduces the energy bandgap and improves the mobility–lifetime product for photogenerated carriers.

1. Introduction

Thin cadmium sulphide (CdS) films have been used as the window material in solar cells. The chemical bath deposition (CBD) technique has been used for the preparation of CdS in a high conversion efficiency (16%) CdS/CdTe solar cell [1].

Among various techniques that can be used for the preparation of thin CdS films (thermal evaporation, chemical spray, electrodeposition and sputtering), CBD is a simple and inexpensive method. In CBD the rate of growth is controllable by pH, temperature and the relative concentrations of the reactants in the bath solution [2–4]. The alkaline bath solution (pH $>$ 9) normally consists of a cadmium salt, thiourea [$SC(NH_2)_2$], NH_4OH and a complexing agent such as NH_4Cl.

Despite the extensive literature data that exist on CBD films of CdS, the optoelectrical properties of these films are not well understood and the reported data show disagreement. This is partly due to the fact that the optoelectrical properties are influenced, to some extent, by the film microstructure, which, in turn, depends on the preparation parameters and postdeposition conditions. The effect of the solution composition and temperature, for instance, on the optical absorption coefficient, resistivity and energy bandgap is considerable [5]. Thermal annealing in different atmospheres reduces the energy bandgap [6, 7]. The electrical resistivity, that can vary over several orders of magnitude, depends not only on the doping level, but also on the film microstructure [8] and thickness [9–12].

For this study CdS films were deposited from a particular bath and their structure, optical and optoelectrical characteristics were measured with the aim of finding the correlation between the optoelectrical and the microstructural parameters. Here we will discuss some experimental

† Author to whom correspondence should be addressed.

0953-8984/00/408745+11$30.00

results on the characteristics of the energy bandgap, the optical absorption tail and the effect of annealing and film thickness on these parameters. The results will be explained in the framework of the film microstructure.

2. Experimental details

Samples were grown on soda-lime glass substrates, in the temperature range 70–90 °C. The alkaline solution (pH $\approx$ 11) consists of $CdCl_2$ (2 mM), thiourea (3 mM), NH_4OH (640 mM) and NH_4C ($\approx$15 mM). The glass substrates were etched in 2% HF (5 min) before deposition. The overall rate of deposition for films with a thickness 80–180 nm could vary from about 0.9 nm min^{-1} at 70 °C to about 8 nm min^{-1} at 90 °C. For the preparation of films thicker than $\approx$200 nm several runs of depositions, each from a fresh solution, were required. The film thickness was determined by using a Tencor surface profiler (Alpha Step 2000) or from its mass (density 4.82 g cm^{-3}).

Optical transmittance measurements were performed in the wavelength range 400–3300 nm using a Varian (Cary-5E) double-beam spectrophotometer. For the measurement of resistivity and spectral response of photoconductivity, two parallel stripes of silver paste were deposited on the film surface. Films used in this study had the as-grown resistivities in the range 10^3–10^4 Ω cm. Annealing in air at 150 °C for 1 h improved the stability of the current under a steady bias but did not appreciably change the resistivity of the films. Annealing at 350 °C, however, increased the resistivity by two to three orders of magnitude and also improved the signal to noise ratio of photoconductivity. The spectral response of photoconductivity, normalized to the incident photon flux, was measured using a PC-controlled set-up. The set-up consisted of a monochromator (Scientech 9050), a mechanical chopper (set to 17 Hz) and a lock-in amplifier (Stanford Research, SR 530). Films structure was determined by the x-ray diffraction (XRD) method using a Siemens D500 diffractometer. The average size of crystallites (grains) was obtained from the Scherrer formula $G = \lambda/(\Delta\theta \cos\theta)$, where $\lambda = 0.154\,06$ nm is the wavelength, $\Delta\theta$ is the angular line width at half maximum intensity and θ is the Bragg angle.

3. Results and discussions

3.1. Microstructure

For structural characterization and the assessment of stoichiometry, x-ray diffraction patterns were obtained for films of different thickness, 100–1000 nm. All the films deposited for this study were stoichiometric and did not show peaks related to elemental cadmium or sulphur. A typical spectrum for a film is compared in figure 1 with that for powder CdS. The film has an average grain size of 76 nm, as determined from the breadth of its (002) peak. Regardless of thickness, films showed a strong preferential orientation of hexagonal (002) planes, parallel to the substrate surface, as shown in figure 1. The interplanar spacing of the (002) planes, d_{002}, and that for the (100) planes, d_{100}, were measured from the positions of the corresponding peaks. The two hexagonal lattice constants $c = 2d_{002}$ and $a = 2d_{100}/\sqrt{3}$ were obtained as 0.6504 nm and 0.4158 nm, respectively, for the film and 0.6722 nm and 0.4142 nm for CdS powder. The film (100) peak could be observed in an extended scale at about $2\theta = 24.7°$. The c/a ratio for the film (1.564) is 3.8% less than that for the powder sample (1.623), where the latter is very close to the ideal value of 1.633 for close-packed hexagonal structures. This implies that the CdS film is under tensile strain along its (002) plane that is parallel to the substrate. Measurements on several films revealed that the magnitude of strain is inversely related to the film thickness.

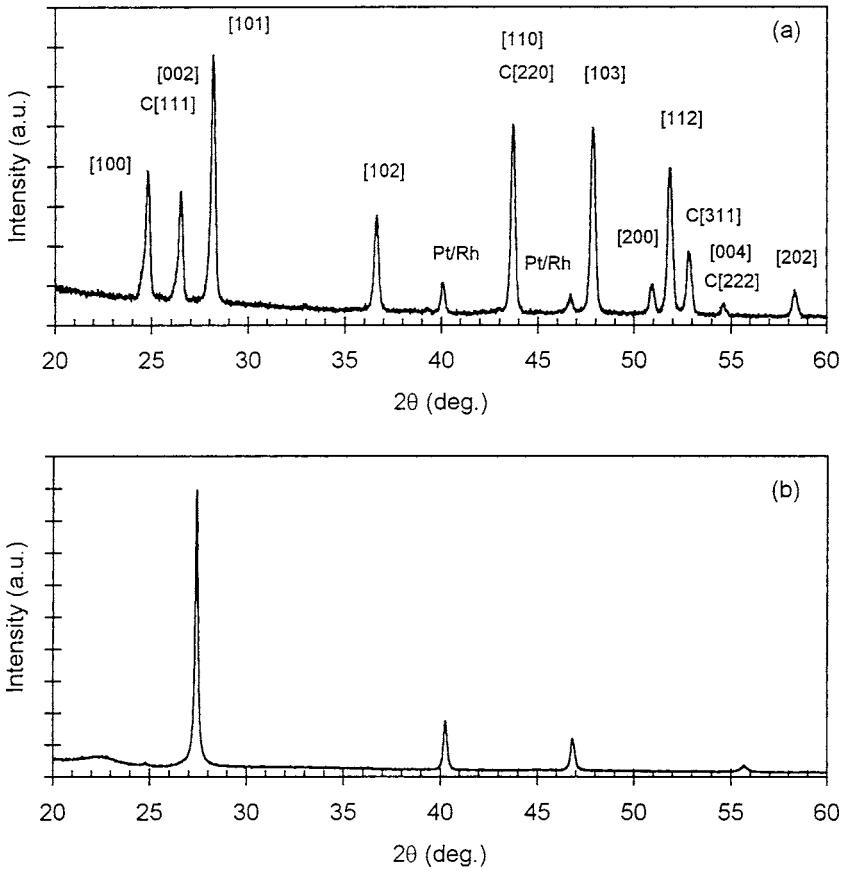

Figure 1. XRD spectrum for (a) commercial CdS powder (Alfa 20108) and (b) a 1000 nm thick film. Labels are for hexagonal directions. Cubic directions are denoted by c. The Pt/Rh peaks are from the sample holder.

3.2. Optical properties

For evaluation of energy bandgap and its variation with the microstructural and annealing parameters, and also for the characterization of absorption tail, the spectrum of the optical absorption coefficient was measured. The optical absorption coefficient, α, of an absorbing film with thickness d deposited on both sides of a glass substrate was obtained from

$$T^{1/2} = \frac{(1 - R_1)(1 - R_2)\ \exp(-\alpha d)}{1 - R_1 R_2\ \exp(-2\alpha d)}. \tag{1}$$

Here, T is the optical transmittance of the structure and R_1 and R_2 are, respectively, the reflection coefficients at the air–film and the film–glass interfaces. Equation (1) is deduced from the original equation that has been used for the characterization of CdTe [13] and SnO_2 films [14], taking into consideration incoherent multiple reflections at interfaces. Both R_1 and R_2 are wavelength dependent parameters through the film and the substrate refractive indices [13, 14]. For calculation of R_1 and R_2 the refractive indices, n, of vapour-grown CdS were used [15]. These data are in good agreement with the dispersion data obtainable from [16]

$$n^2 - 1 = 99.96/(24.01 - E^2) \tag{2}$$

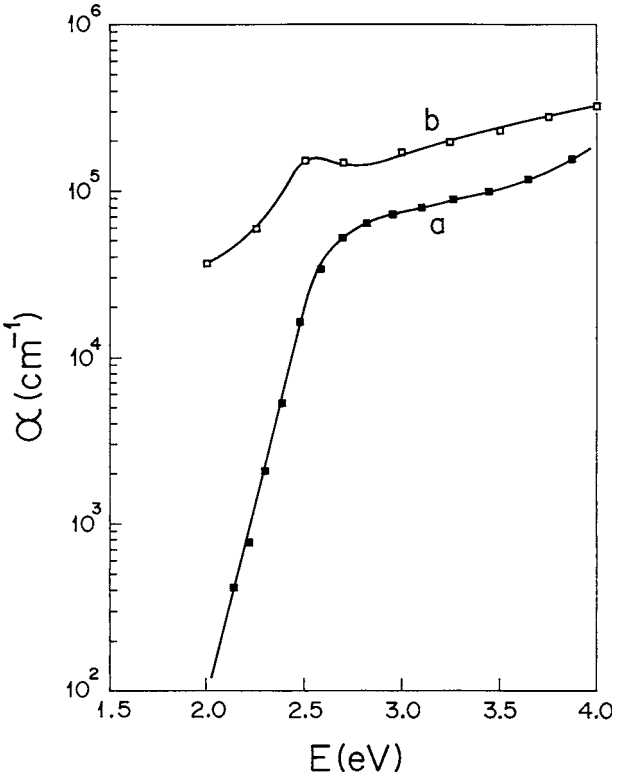

Figure 2. The spectrum of absorption coefficient for a 146 nm CdS film (a) and for a CdS platelet [16] (b). E is the photon energy.

where E is the photon energy in eV. Figure 2 compares the measured values of α for a 146 nm thin film with that for a single crystal. The optical absorption coefficient of the thin-film sample is in fair agreement with reported values [5] and is slightly smaller, in the spectral range shown, than that for the single crystal. The latter data have been obtained from the Kramers–Kronig analysis of reflectance results on the platelet of vapour-grown CdS. In the photon energy range 2.5 eV $< E <$ 3.1 eV, a plot of $(\alpha E)^2$ against E yields a straight line as shown in figure 3. The horizontal intercept of this line yields the direct energy bandgap of the sample as 2.51 eV, which is in an acceptable range [6, 7].

The absorption coefficient of the thin-film sample shows a tail for sub-bandgap photon energies. The Urbach energy E_u associated with this tail can be measured from the fit of data to [17]:

$$\alpha = \alpha_0 \exp[(E - E_0)/E_u] \tag{3}$$

where α_0 and E_0 are two constants. E_0 coincides, roughly, with the energy of the lowest free exciton at zero lattice temperature. The E_u value that determines the steepness of the Urbach tail depends on temperature through electron/exciton–phonon interaction and also depends on the structural disorder of the sample. According to the Cody model [18]

$$E_u = \frac{E_p}{2\sigma_0}\left[X + \coth\left(\frac{E_p}{2kT}\right)\right] \tag{4}$$

where E_p is the phonon energy, σ_0 is a material-dependent parameter and X is a measure of structural disorder. Here, X is the ratio of the mean square deviation of atomic positions, caused

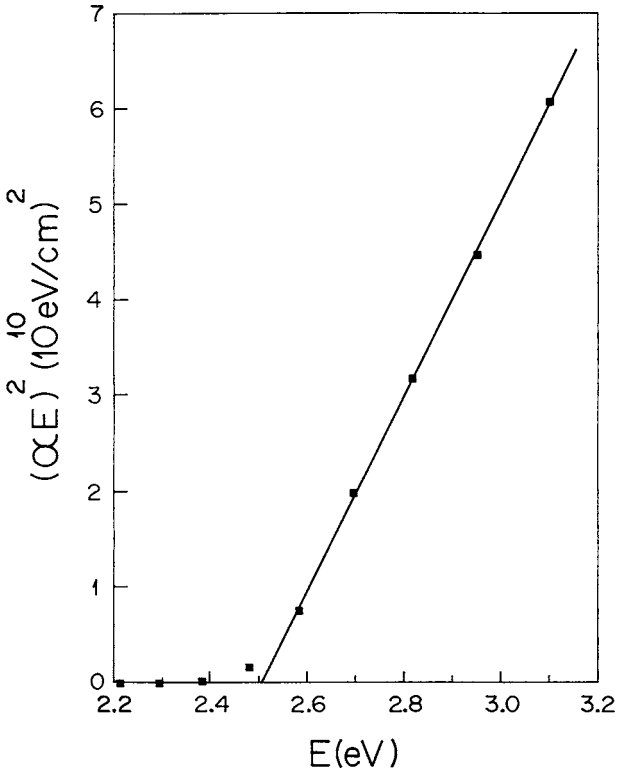

Figure 3. The plot of $(\alpha E)^2$ against photon energy E for the thin-film sample of figure 1. The horizontal intercept of the straight-line fit measures an energy bandgap $E_g = 2.51$ eV.

by disorder, to the zero-point uncertainty in the atomic positions. From figure 2, $E_u = 94$ MeV was obtained. This yields a disorder parameter $X = 6.72$, using $E_p = 25$ meV and $\sigma_0 = 1.19$. The last two parameters were determined, for a similar sample, from the fit of equation (4) to the E_u values measured at different temperatures [19]. Further discussion on the disorder parameter and its variation with annealing is given in section 3.5.

3.3. Spectral response of photoconductivity

The characteristics of energy bandgap and the absorption tail can also be evaluated from the measurement of the spectral response of photoconductivity. This is easier to measure than the optical absorption coefficient. Figure 4 shows the spectral response of photoconductivity, R, normalized to the photon flux for a sample after being annealed in air at different temperatures. Annealing in air increases the dark resistivity of the films and, hence, reduces the random fluctuation of dark current (Johnson noise), causing an appreciable improvement in the signal-to-noise ratio of the spectral response. The plots in figure 4 do not show a maximum, indicating that the recombination of photogenerated carriers by surface states is negligible [20]. For a film thickness, d, much greater than the diffusion length of photogenerated carriers, a condition which is normally satisfied in polycrystalline films, $R \propto (1 - e^{-\alpha d})$ [21]. R becomes independent of α and, thus, of E when $\alpha d \gg 1$. Examination of α values for the as-deposited CdS film shown in figure 2 and using $d = 146$ nm reveals that such a condition is not fulfilled and, thus, R increases steadily in the range $E > E_g$, as seen in figure 4, plots

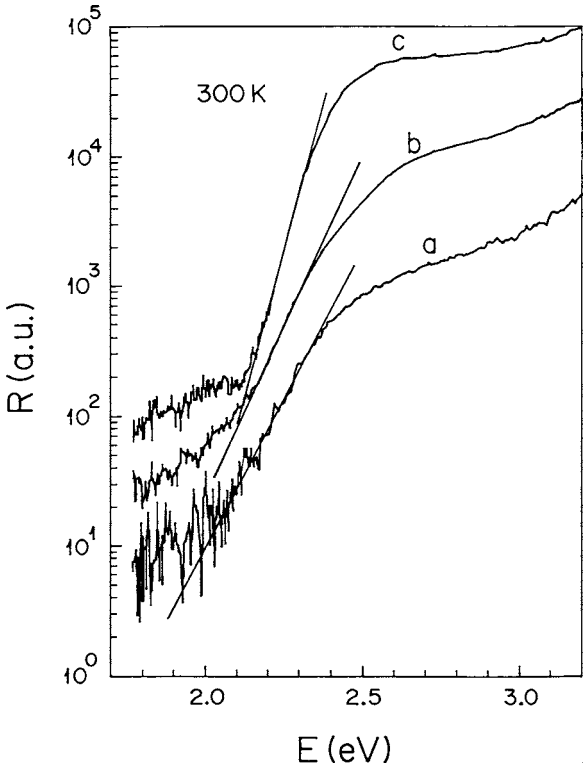

Figure 4. The spectral response of photoconductivity, R, for the thin-film sample of figure 2 after annealing at 150 °C (a), 200 °C (b) and 350 °C (c). Annealing was for 1 h in air. The Urbach energy is 94, 88 and 50 MeV for plots a, b and c, respectively. For clarity, these plots are shifted arbitrarily along the R axis.

(a) and (b). However, after annealing the sample at 350 °C, R becomes nearly independent of E for $E > 2.6$ eV. This indicates that annealing at 350 °C has apparently increased α to its value for the bulk sample ($\approx 2 \times 10^5$ cm^{-1}, figure 2) for which $\alpha d \approx 3$. This increase in α is apparently associated with the absorption of photons by the extended states that are developed as the result of annealing, as will be discussed in more detail in section 3.6. In the low-photon-energy range ($\alpha d < 1$), R becomes proportional to α and can be used, instead, for the characterization of the Urbach tail and the measurement of bandgap energy. Figure 5 shows $(RE)^2$ against E curves corresponding to the plots in figure 4. The increase of the slope of these plots with annealing, at a temperature exceeding 150 °C, is likely due to the enhancement of the lifetime–mobility product of excess carriers. This can be associated with the reduction of the height of the grain boundary potential barrier. The energy bandgap is measured to be 2.50 eV for samples annealed at 150 and 200 °C, in agreement with 2.51 eV obtained from the α values in figure 3. Annealing at 350 °C, however, reduces the bandgap to 2.39 eV. The Urbach energy measured from plot (a) in figure 4 is 94 meV. This is exactly the same as that obtained from α values in figure 2, plot (a). For photon energies below the Urbach tail region, the R–E plots show another tail that is likely related to transitions between the bandgap levels and the energy bands. The identical results obtained for E_u and E_g from the spectra of α and R, confirm the validity of the relationship between R and α, as quoted above.

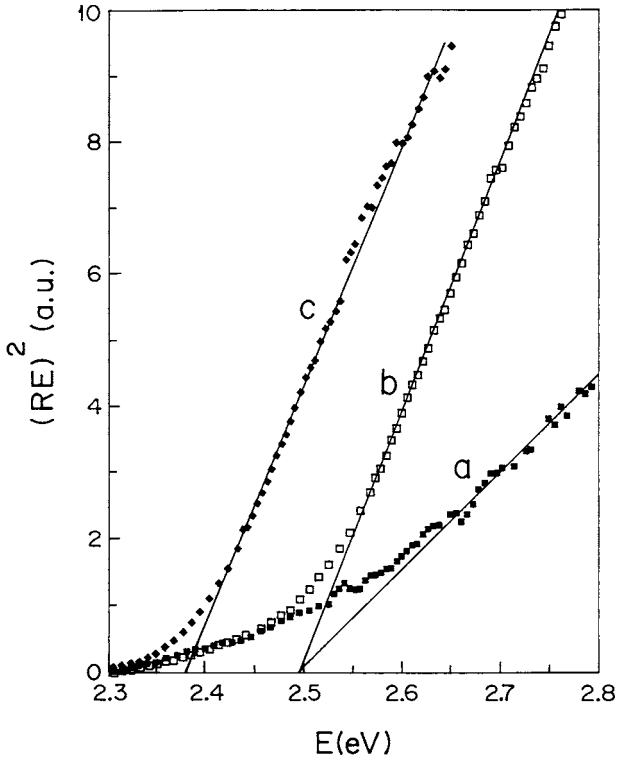

Figure 5. $(RE)^2$ against E plots corresponding to the curves of figure 4. The energy bandgap is measured to be 2.50 eV for the samples annealed at 150 °C (a) and 200 °C (b). The bandgap for the sample annealed at 350 °C (c) is 2.38 eV. R is the spectral response and E is the photon energy.

3.4. The effect of film thickness on energy bandgap

Figure 6 shows the optical bandgap of several films with different thickness, before and after being annealed at different temperatures. The bandgap values were determined from the $(\alpha E)^2$ against E plots. These values were about 26 meV, on the average, greater than those obtained from the spectral response measurements. Regardless of the annealing temperature, bandgap shows a minimum for a thickness of 700–900 nm. For the preparation of films thicker than 200 nm, several deposition runs had to be performed, each from a fresh solution. The rate of deposition is high at the beginning of each deposition run and decays as the film grows. This is due to the depletion of reactants from the bath solution. Therefore to deposit a thick film in a reasonable time period, the average rate of deposition was increased by increasing the number of layers and reducing the period for each deposition run. The average grain size for most of the samples of figure 6 is shown in figure 7. The average rate of deposition for these samples varies monotonically from 2.4 to 5.2 nm min^{-1} in increasing order of thickness. The average grain size increases appreciably with increasing film thickness and, on the other hand, decreases as the rate of deposition increases. Due to these two opposite trends, a maximum is observable in figure 7, in the same thickness range of 700–900 nm as for the minima in figure 6. This implies that there is an inverse relationship between the energy bandgap and the grain size. On the other hand, measurements revealed a direct relationship between the grain size and the d_{002} value (more tensile strain in films with smaller grains). As a result, an approximate relationship was derived as $\Delta E_g/E_g = -\beta \Delta d_{002}/d_{002}$ ($\beta \approx 5$–8), which relates

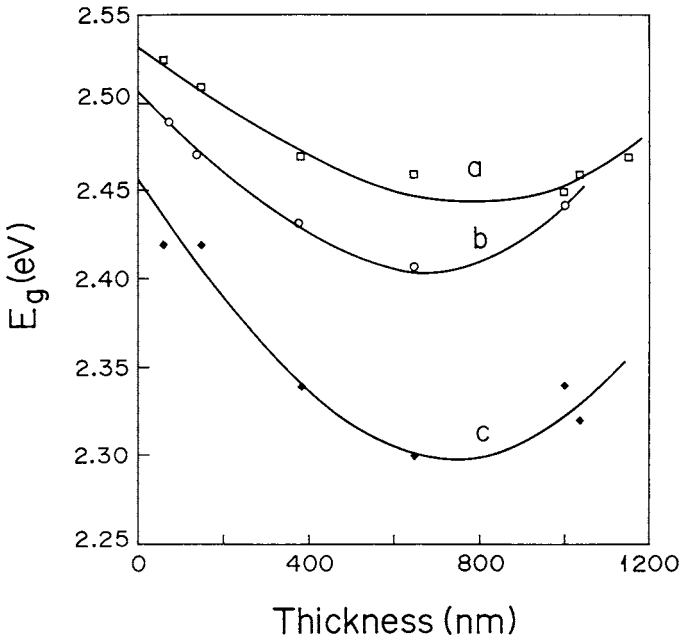

Figure 6. The optical bandgap of CdS films with different thickness before (a) and after heat treatment in air for 1 h at 200 °C (b) and 350 °C (c).

the relative change of bandgap to the extent of strain. The effect of grain size on the bandgap, as the result of electron confinement in grains [22], is negligible in our samples for which grains are larger than 10 nm. Therefore, we attribute the thickness dependence of bandgap shown in figure 6 to the effect of lattice strain.

3.5. The effect of annealing on disorder parameter

Table 1 summarizes the effect of annealing on the disorder parameter X for several samples. X was obtained from equation (4) using $E_p = 25$ meV, $\sigma_0 = 1.19$ and measuring E_u from the spectral response of photoconductivity, as in figure 4. The results revealed that annealing at temperatures below 200 °C has negligible effect on X. Annealing at 350 °C, however, decreases the disorder parameter appreciably. The decrease of X with annealing is likely related to the reduction in the density of defects in grain boundaries. Annealing, however, does not cause an appreciable grain growth, which can be detected from the breadth of XRD peaks. The lattice deformation in these films that have columnar grains is likely due to the fact that the grain boundaries with a highly defective structure apply a tensile strain on grains, parallel to the substrate surface. This decreases the lattice constant c, along the [002] direction. Annealing at 350 °C reduces the density of defects and, thus, the extent of disorder in grain boundaries. This, in turn, relaxes the strain and increases d_{002} towards its stress-free value. The relative increase in d_{002}, which is a measure of strain relaxation with annealing at 350 °C, is shown in figure 8. The strain relaxation and the relative decrease in disorder parameter are compared for several samples in table 1. Both seem to be more effective in thicker films with larger grains where the bulk properties of grains dominate the grain-boundary constrictions and also where the bulk of the film is less influenced by the constrictions imposed by the substrate.

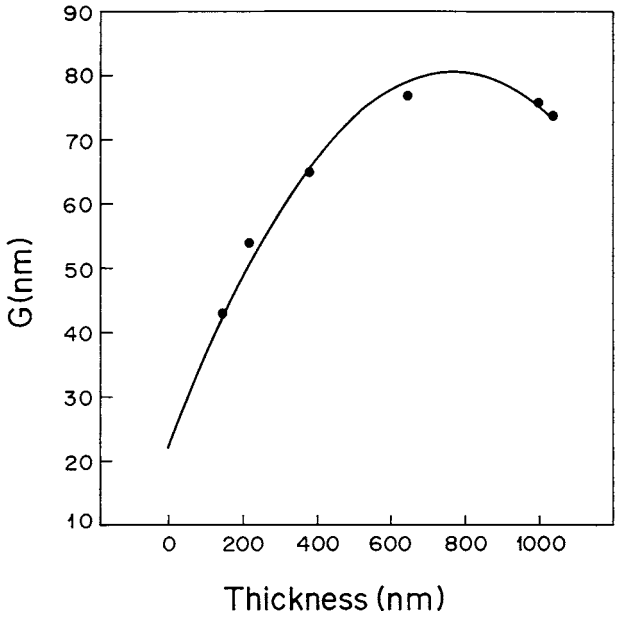

Figure 7. The average grain size as a function of film thickness. The average rate of deposition for films is 2.43, 3.94, 3.2, 3.3, 4.2 and 5.2 nm min^{-1}, in the increasing order of film thickness.

Table 1. The disorder parameter, X, measured at 300 K for different films that have been annealed for 1 h in air at different temperatures; d is the film thickness; $(\Delta X/X)$ and $\Delta d_{002}/d_{002}$ are, respectively, the relative change in the disorder parameter and in the (002) interplanar spacing of as-deposited samples due to annealing at 350 °C. The X values for the as-deposited and the 150 °C annealed samples are taken to be the same.

Sample	d(nm)	X 150 °C	X 200 °C	X 350 °C	$\Delta X/X$	$\Delta d_{002}/d_{002}$
G11	146	6.7	6.1	2.5	−1.7	0.9×10^{-3}
G31	647	9.7	7.2	2.5	−2.8	1.8×10^{-3}
G21	1037	9.1	8.1	1.7	−4.3	2.4×10^{-3}

3.6. The effect of annealing on bandgap energy

Figure 6 shows the energy bandgap of several samples with different thickness before and after being annealed at 200 and 350 °C for 1 h. The dependence of energy bandgap on the film thickness has already been discussed. Regardless of film thickness, annealing reduces the bandgap energy. Annealing increases the (002) interplanar distance by relaxing the grain-boundary-related tensile strain, as discussed before. Figure 8 shows the relative increase of d_{002} in different samples as the result of annealing at 350 °C. The value of $\Delta d_{002}/d_{002}$ increases with the film thickness, in the range 0.06–0.3%. However, the relative decrease of energy bandgap as the result of the same annealing process (350 °C for 1 h) is about 4–6% and independent of the film thickness. Therefore, the effect of annealing on energy bandgap is unlikely to be due to the partial relaxation of strain.

Annealing in different atmospheres such as H_2, Ar, air and sulphur is known to reduce the energy bandgap of CdS films [6, 7]. Some authors attribute this to the phase change from hexagonal to cubic [7], although the difference of energy bandgap in the two phases is only

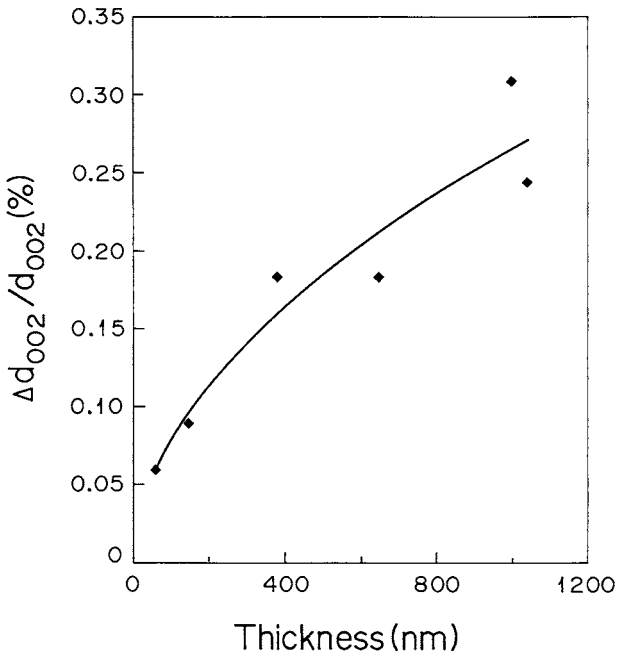

Figure 8. The relative increase of the interplanar spacing of (002) planes (parallel to the substrate) for films with different thickness, as the result of annealing in air at 350 °C for 1 h.

30 meV (2.48 eV for hexagonal and 2.45 eV for cubic) [23]. The enlargement of the CdS cubic cell, as a result of annealing in sulphur vapour, is held responsible for the decrease of bandgap from 2.42 eV to 2.31 eV [24]. The reduction of energy bandgap in our samples with annealing can be explained by the Tsai model [25] in which the density of extended states increases and bridges the conduction band to a donor level. The range of the reduction in energy bandgap with annealing that is deducible from figure 6 is consistent with this model, considering that the dominant donor level in CBD-grown films is located 0.15–0.18 eV below the conduction band edge [5]. Here, the extended energy states are assigned to the bulk of grains in contrast to the grain-boundary-related extended states that determine the steepness of the absorption tail, and their density decreases with annealing.

4. Conclusions

This study contributes to the literature some new results as summarized in the following. Thin films of CdS grown on glass by the CBD technique have a strained lattice; the interplanar distance of (002) planes is smaller than the bulk value. The magnitude of strain which depends on the film thickness, through the grain size, is accountable for the variation of bandgap energy with the film thickness. Annealing in air improves the steepness of the Urbach tail as the result of reducing the grain-boundary defect density. Annealing lowers the energy bandgap due to the development of grain-related extended states. Annealing also relaxes the lattice strain and improves the mobility–lifetime product for the photogenerated carriers.

Acknowledgments

The support of the Research Administration of Kuwait University under project SP057 is gratefully acknowledged.

References

[1] Britt J and Ferekides C 1993 *Appl. Phys. Lett.* **62** 2851
[2] Ortega-Borges R and Lincot D 1993 *J. Electrochem. Soc.* **140** 3464
[3] Oladeji I O and Chow L 1997 *J. Electrochem. Soc.* **144** 2342
[4] Lanning B R and Armstrong J H 1992 *Int. J. Solar Energy* **12** 247
[5] Dona J M and Herrero J 1997 *J. Electrochem. Soc.* **144** 4091
[6] Tomas S A, Vigil O, Alvarado-Gil J J, Lozada-Morales R, Zelaya-Angel O, Vargas H and Ferreira da Silva A 1995 *J. Appl. Phys.* **78** 2204
[7] Hernandez L, de Melo O, Zelaya-Angel O and Lozada-Morales R 1994 *J. Electrochem. Soc.* **141** 3238
[8] Grovenor C R M 1989 *Microelectronic Materials* (Bristol: Hilger)
[9] Chaudhuri S and Pal A K 1993 *Electrical Properties of Polycrystalline II–VI Compound Semiconductor Films* ed M Jain (Singapore: World Scientific) p 561
[10] Kazmerski L L, Berry W B and Allen C W 1972 *J. Appl. Phys.* **43** 3515
[11] Wilson J I B and Woods J 1973 *J. Phys. Chem. Solids* **34** 171
[12] Kazmerski L L 1974 *Thin Solid Films* **21** 273
[13] Rakhshani A E 1997 *J. Appl. Phys.* **81** 7988
[14] Rakhshani A E, Makdisi Y and Ramazaniyan H A 1998 *J. Appl. Phys.* **83** 1049
[15] Ward L 1991 *Handbook of Optical Constants of Solids II* ed D Palik (San Diego, CA: Academic) p 579
[16] Wemple S H and Didomenico M Jr 1971 *Phys. Rev.* B **3** 1338
[17] Kurik M V 1971 *Phys. Status Solidi* a **8** 9
[18] Cody G D, Tiedje T, Abeles B, Brooks B and Goldstein Y 1981 *Phys. Rev. Lett.* **47** 1480
[19] Rakhshani A E 2000 *J. Phys. C: Solid State Phys.* **12** 4391
[20] Bube R H 1992 *Photoelectric Properties of Semiconductors* (Cambridge: Cambridge University) p 21
[21] De Vore H B 1956 *Phys. Rev.* **102** 86
[22] Mathieu H, Richard T, Allegre J, Lefebvre P and Arnaud G 1995 *J. Appl. Phys.* **77** 287
[23] Mendoza-Galvan A, Martinex G and Lozada-Morales R 1996 *J. Appl. Phys.* **80** 3333
[24] De Melo O, Hernandez L Zelaya-Angel O, Lozado-Morales R and Becerril M 1994 *Appl. Phys. Lett.* **65** 1278
[25] Tsai C T, Chuu D S, Chen G L and Yang S L 1996 *J. Appl. Phys.* **79** 9105